J.-M. Le Tensorer, R. Jagher & M. Otte (eds.). *The Lower and Middle Palaeolithic in the Middle East and Neighbouring Regions.*
Basel Symposium (May 8-10 2008).
Liège, ERAUL 126, 2011, p. 249-261.

CHRONOMETRIC AGE ESTIMATES FOR THE SITE OF HUMMAL (EL KOWM, SYRIA)

Daniel RICHTER[1], Thomas C. HAUCK[2], Dorota WOJTCZAK[3], Jean-Marie LE TENSORER[3] & Sultan MUHESEN[4]

[1] Max-Planck-Institute for Evolutionary Anthropology, Department of Human Evolution, Leipzig, Germany, drichter@eva.mpg.de
[2] Institut für Ur- und Frühgeschichte der Universität zu Köln, Germany, thomas.hauck@uni-koeln.de
[3] Institute for Prehistory and Archaeological Science (IPAS) University of Basel, Switzerland, dorota.wojtczak@unibas.ch, jean-marie.letensorer@unibas.ch
[4] Université de Damas and Qatar Museums Authority, smuhesen@qma.org.qa

Introduction

Thermoluminescence (TL) and Optically Stimulated (OSL) ages for the sequence of Hummal (El Kowm, Syria) are presented. Because of disequilibria in the U-decay chain the external γ-dose rates cannot be assumed as constant over burial time and have to be modelled. The resulting model ages are significantly different for the Mousterian layer '5g' and the Hummalian layer '6b East'. While the age estimates for layer '6b East' are rejected as unreliable, a provisional age for the Mousterian occupation of 100 ka is given. The TL age estimates on heated flint from another Hummalian layer (α-h base) do not suffer from significantly different model ages and compare favourably with an age of 200 ka with other chronometric ages for similar blade-rich assemblages in the Levant. The OSL age for sediment sample layer '15b', located lower in the middle of the sequence at Hummal, is apparently underestimating the age, when the other results as well as the chronostratigraphical sequence is taken into consideration. The post-depositional formation of authigenic quartz crystals as well as secondary silica coatings are suggested as a likely source for the underestimation, and the OSL age result is therefore rejected for layer '15b'.

Presentation of the Hummal site

The spring site of Hummal is located in Central Syria, near the village of El Kowm between the Euphrates basin and the desert steppe. The site of Hummal is a prominent mound at an artesian spring which was responsible for piling up of sediments during the Quaternary. The impressive 20 m stratigraphy comprises more than 25 geological units preserving a large number of archaeological levels. It covers a long period of time ranging from the Lower Palaeolithic (Oldowan) to the Upper Palaeolithic over more than one million years. The mound is the eponymous site for the technocomplex of the Hummalian.

As of yet, the stratigraphy is the longest and most important cultural sequence known in an arid landscape in the Middle East. It is therefore especially important to provide a chronostratigraphy not only based on comparisons and dating results gathered elsewhere, but rather on chronometric age estimates obtained directly for the sequence. The general chronostratigraphical sequence of the Near East is heavily based on the long stratigraphy of Tabun (Bar-Yosef & Meignen 2001; Mercier & Valladas, 2003; Mercier *et al.* 1995b, 2000; Porat *et al.* 2002), but the sequence at El Kowm provides in principle the unique opportunity for verification.

The stratigraphy and an extensive description of the geological and archaeological sequence of Hummal (Hauck *et al.* 2010; Le Tensorer *et al.* 2003, 2007; LeTensorer 2004) are given in this volume (Le Tensorer *et al.* 2011).

The Lower Palaeolithic sequence at the base of Hummal (Units G and F) comprises Oldowan-like assemblages (Layers 21-15; Wegmüller 2011) which are followed by two "Acheuleo-Tayacian" assemblages (layers 14-13) consisting of unspecific flakes, few flake tools and two handaxes (Le Tensorer *et al.* 2011).

The Early Middle Palaeolithic (Units E and D) is represented by Yabrudian artefacts in layers 12 to 8, followed by a drastic change in lithic production towards blades and elongated points as characteristic hallmarks. Such a particular assemblage was defined as Hummalian by Francis Hours (1982), based on his initial study of unstratified finds (layer Ia) from the site. This technocomplex is represented in the new excavations in primary (layers 6a, 6b, 6c, 7a, 7c) and in secondary context (α-h). The latter assemblage has been recovered from the sandy filling of a dolina. All the materials attributed to the Hummalian show a strong technological relationship (Wojtzcak 2011). Based on geological observations (Le Tensorer 2004), it is assumed that the material of layer 'α-h' from the dolina filling corresponds to a stratigraphic position between layer 8 (Yabrudian) and layer 7 (Hummalian). While the lithics from the sands have fresh edges, despite a secondary silica cover (Masson 1982; Shackley 1988), the lithics from layer 6b are uniformly patinated and often broken which suggests surface exposure and trampling (Wojtczak 2011). While the dolina filling represents a catastrophic depositional event, the depositional history of the sediment covering the artefacts in layer 6b is not clear and it might have accumulated over an extended period of time. All these Hummalian assemblages fit well into the generally observed development of blade-industries in the Middle East at the beginning of the

Middle Palaeolithic, e.g. at Tabun D or at Hayonim, Abou Sif in Palestine (Meignen 2007; Neuville 1951).

The following 4 m deep Mousterian sequence (Unit C) with more than 30 archaeological levels is mainly composed of detrital carbonate deposits in alternation with poorly developed soil formations and evaporitic sediments, such as gypsum-clay accumulations. Based on the archaeological material, the sequence can be grouped into three industry types (Hauck 2010, 2011). A Middle Levantine Mousterian of Tabun C type is found at its base. The upper two Mousterian industries show a clear focus on Levallois point production with variable reduction strategies, and hence, can be assigned to a Late Levantine Mousterian of Tabun B type. Two human remains of unspecified species (Neanderthal or archaïc *Homo sapiens*) were discovered in layers 5a4 and 5b1 (Hauck 2010).

A hiatus in the sedimentation is capping the Mousterian horizons from a period of colluvial formation, which contains an Upper Palaeolithic (probably Levantine Aurignacian), underlying an impressive Holocene deposit with traces of proto-historic and historic occupations.

Previous chronometric age estimates for Hummal

Earlier attempts to provide chronometric age estimates for the site of Hummal are limited to thermoluminescence dating of heated flint (Ancient TL date list 1988), with three dates each from a Yabrudian layer Ib (as defined in the 1983 stratigraphy) and a late Middle Palaeolithic layer VIb (tab. 1). While the position of the former layer to the present stratigraphy remains unclear, layer VIb (profile P3 East) corresponds to layer '6b East' (now attributed to Hummalian), from which TL data on burned flints is presented in this paper.

The results for layer Ib (Yabrudian) with a context age of 160 ± 22 ka were critiqued by Mercier and Valladas (1994) for probably not being based on reliable external dosimetry. They noted a discrepancy of the dosimeter results with data from Hennig and Hours (1982), and their analysis of a sediment sample from layer '6b' with γ-ray spectrometry found the U-decay chain not being in secular equilibrium. This indicates an overestimation of the dosimetry and the ages therefore have to be regarded as minimum ages (Mercier & Valladas 1994). Furthermore, the results for layer 6b were additionally challenged because of a low correction of sediment moisture, despite the occurrence of deposits indicating the presence of water at the site. This lead to an additional overestimation of the external γ-dose rate for these samples (Mercier & Valladas 1994). Additionally, the techniques used to generate these dates appear not to take into consideration the supralinearity, and the palaeodoses therefore are underestimated, which results in a further underestimation of the age. The context age of the three heated flint samples from the layer VIb of 104 ± 9 ka (Ancient TL date list, 1988) was subsequently wrongly attributed to Mercier *et al.* (1995a) by Herz & Garrison (1998).

Further attempts were made by dating the formation of secondary carbonates from a conglomerate of not well consolidated travertines of a Yabroudian context (layer Ib, 1983 stratigraphy) at Hummal (Hennig & Hours 1982), which gave an age estimate of 138-179 ka (1-σ). This result is based on the assumption of equal initial activities of ^{230}Th and ^{232}Th (Hennig & Hours 1982). However, as the sediment is described as a conglomerate, the formation of these secondary carbonates has to be suspected of not being related to the archaeological event of the deposition of the Yabroudian. Furthermore, not well consolidated secondary carbonates are prone to contamination and, with respect to the archaeology, can therefore be considered as minimum ages at best. Tentative ESR dating of this travertine provided an age considerably smaller than the U–series result and was considered as unreliable (Hennig & Hours 1982).

sample ID	layer	age (ka)	±	archaeology
235 1b (i)	Ib	180	25	Yabrudian
235 1b (ii)	Ib	145	20	Yabrudian
235 1b (ii) *	Ib	160*	23	Yabrudian
(Ox85TLfg)	**Ib**	**160**	**22**	**context age Yabrudian$**
235 6b (i)	VIb	97	8	Late Mousterian (now Hummalian)&
235 6b (iii)	VIb	105	9	Late Mousterian (now Hummalian)&
235 6b (v)	VIb	112	10	Late Mousterian (now Hummalian)&
235 6b	**VIb**	**104**	**9**	**context age Hummalian&**

Table 1 - Previous TL dating results of heated flint (data from Ancient TL date list, 1988). * The actual age of this sample is 165±23 ka according to the data given in the technical part of the same report, which results in a non-significant increase of the calculated context age; $ not in situ; & in situ and corresponding to layer '6b' of the present stratigraphy, now attributed to a Hummalian industry; designation of layers according to the 1983 stratigraphy.

Thermoluminescence (TL) Dating of heated flint artefacts

TL dating of heated flint artefacts determines the timing of the last heating of rock material, and thus the time elapsed since lighting a fire. It is one of the few instances where chronometric dating can provide an age estimate of a prehistoric activity directly (Richter 2007). Natural fires are frequent (see discussion in Alperson-Afil *et al.* 2007), but heat penetration of natural fire into sediment is low (Bellomo 1993). Therefore any rock material which is covered by a few centimetres of sediment only is not heated to an extent that would allow TL dating (Richter 2007). Given the suspected antiquity of the site, a delayed lighting of a fire by a subsequent occupation having been responsible for heating the artefacts, is considered as being not significant with respect to the resolution of the TL-dating method. Natural fires can be considered as unlikely being the responsible agent for the heating, because of the geomorphological position and that only a fraction of the lithics from Hummal show traces of heating. The fire therefore can be attributed to human activities, which provides the association of the sample and the event dated.

The method of TL dating of heated flint artefacts is based on the accumulation of metastable charges (palaeodose) in the

crystal lattice by ionizing radiation since the last heating of the rock (Aitken 1985). Such charges in the crystal lattice of minerals are caused by the ionizing radiation due to the decay of radioactive elements from the surrounding sediment (external dose) and the sample itself (internal dose), as well as secondary cosmic rays (external dose). This omnipresent ionization causes a radiation dose (palaeodose or P) to accumulate in the crystal in the form of electrons in excited states. For dating application only electrons in metastable states are targeted, which are resident over periods of time much longer than the anticipated age (approximately 50 Ma after Wintle & Aitken 1977). Detailed descriptions of the principles of luminescence dating methods can be found elsewhere (Aitken 1985, 1998; Bøtter-Jensen *et al.* 2003; Wagner 1998) and a general account of TL dating of lithics is given in Richter (2007).

Samples for thermoluminescence dating

Artefacts showing macroscopic traces of heating, like potlids, craquelation, crenation, reddening (Richter 2007), were submitted for TL-analysis. The majority is not suited for TL dating because temperatures achieved were too low to allow TL dating. From this ongoing study we here report on 2 samples from layer '5g' belonging to the lower Mousterian sequence, and 12 samples from layers '6b-East' (the eastern section of layer 6b) and 'α-h base', both attributed to the Hummalian technocomplex.

Layer '5g' at the base of the western Mousterian sequence consists of detritic sands and carbonate clasts, in which numerous lithic artefacts were discovered. Variable degrees of patination and trampling are observed on some of the artefacts, which lead to the conclusion of layer '5g' being a palimpsest, representing a mixture of more than one occupation (Hauck 2010). However, micromorphological data indicate a rather rapid burial of layer '5g', and hence, the time slot of its formation does not seem to be extensive (Meyer 2001).

The artefacts from layer '6b-East' are heavily and homogenously patinated and, probably as the result of trampling, often broken and/or edge-damaged. Geoarchaeological investigations indicate an intermittent sedimentation over an erosive base, but the level is clearly not a reduction horizon (Meyer 2008). Archaeologically the material is a homogenous Hummlian industry with no natural intermixture of older materials and most likely the result of successive human occupations (Wojtczak 2011).

Layer 'α-h base' was found within a dolina filling, which consists of pure, mostly unstructured sands and represents a catastrophic depositional event. However, the edges of the artefacts are fresh, despite a post-depositional coating with silica (Masson 1982; Shackley 1988). Based on stratigraphic reasons, it is believed that the time between original sedimentation and redeposition of the 'α-h base' material is marginal (Le Tensorer 2004). Stratigraphic observations indicate a deposition of layer '6b East' after layer 'α-h base'. Therefore the difference in the dose rates as measured today, and the actual average dose rate (i.e. the sum of the doses delivered in the first and secondary deposition, see below) are assumed to be negligible. Therefore TL dating should provide a reasonable approximation of the age of the heating event. However, it has to be stressed that any results under such circumstances have to be considered carefully.

Method of thermoluminescence dating

The palaeodose (P) is a function of the dose rate ($\dot{D}$ the ionizing radiation per time unit), which provides the clock for the dating application, i.e. the time scale the crystal was exposed to the omnipresent radiation. Exposure to light or elevated temperatures causes the electrons to relax to a ground state, sometimes by emitting a photon, which is the luminescence. If the temperature is high enough (> ~400 °C) the drainage is sufficient to relax all electrons relevant to the luminescence method used, i.e. the clock is set to zero by this event. After cooling the radiation dose starts to accumulate again and as a consequence the intensity of the luminescence signal (number of photons) increases with the total absorbed dose (P) in a crystal and is therefore a function of exposure time to radiation.

The age is obtained by the ratio of the palaeodose to the sum of a series of dose-rates under the assumption of the constancy of the ionizing radiation (dose-rate) over the entire burial time (Aitken 1985) (fig. 1). The denominator $\dot{D}$ of the age formula consists of two sets of parameters, the internal ($\dot{D}_{internal}$) and the external dose rates $\dot{D}_{external}$). Any variability of any of the parameters of $\dot{D}$ through time makes it difficult to estimate the age of a heated flint (e.g. Richter 2007). All parts of the samples which are considered to be potentially geochemical unstable, like cortex or patinated portions, are carefully removed with a water-cooled diamond saw from the flint samples prior to TL-dating. The internal dose-rate ($\dot{D}_{internal}$), which is measured with Neutron Activation Analysis (NAA) on a subset of the crushed sample, is thus considered as being constant over the time-span of interest. This is an advantage of heated flint TL-dating over most other dosimetric dating methods, and increases the accuracy for any age estimate. However, the major uncertainty in TL-dating of heated flint usually derives from the estimates of uncertainties associated with the ionizing radiation from the surrounding sediment ($\dot{D}_{external}$) which is measured by either gamma ray spectrometry or insertion of dosemeters in the sediments for a specified period of time. In order to simplify the estimation of $\dot{D}_{external}$, and thus increase the precision of an age estimate, each sample is carefully stripped of its outer 2 mm surface area (approximately the range of b-radiation from isotopes contained in the surrounding sediment).

Of major concern in dosimetric dating is the assumption of the stability of the dose rates over burial time. While this is certainly valid for the internal dose rate of the heated flints because only unaltered parts are used (i.e. not patinated) it has to be verified for the external dose rates, (i.e. external γ only in the case of flints) by HPGe γ-spectrometry. However, only the present state can be determined and past changes (i.e. disequilibrium in the decay chains of Th and U) are difficult to detect and to model, especially as they could have occurred repeatedly. Because of size limitations only the smaller sediment particles can be analysed in the laboratory by HPGe γ-ray spectrometry (i.e. rocks and larger artefacts are not included). The results are therefore not necessarily representative if the

$$age_{(ka)} = \frac{P_{(Gy)}}{\dot{D}_{(Gy \cdot a^{-1})}} = \frac{P}{\dot{D}_{(internal)} + \dot{D}_{(external)}} = \frac{P}{(\eta \dot{D}_{\alpha} + \dot{D}_{\beta} + \dot{D}_{\gamma}) + (\dot{D}_{\gamma} + \dot{D}_{cosmic})}$$

Figure 1 - Age formula after Aitken (1985), palaeodose (P) is expressed in Gy, dose rates ($\dot{D}$) in Gy per time unit (usually in a or ka).

sediment contains abundant rocks and artefacts ("lumpy" after Schwarcz 1994).

TL measurement parameters and sample preparation

Because the luminescence signal of some samples from Hummal is at the onset of saturation, the palaeodose on the 90-160 μm fractions of the crushed flint material (after the removal of the outer 2 mm) was obtained by a multi-aliquot-additive-regeneration (MAAR) slide protocol (fig. 6). A comparison of data sets which could be analysed using a standard linear approximation approach revealed no significant differences in palaeodose results at the confidence level of 68%. Therefore a single analytical procedure which is appropriate for all samples was used.

In this slide approach the (linear) alpha contribution to the natural and additive TL-signals is subtracted and the TL data is described by quadratic functions and shifted along the dose axis (Mercier 1991; Valladas & Gillot 1978) with scaling of the regeneration curve (after Sanzelle *et al.* 1996). This procedure is similar to the Australian Slide Method (Prescott *et al.* 1993) and almost identical to the one employed for TL-dating of heated flints of approximately the same age at Hayonim by Mercier *et al.* (2007). An iteration procedure then corrects for the underestimation of the alpha contribution for samples at the onset of saturation, which is based on a linear approximation (after

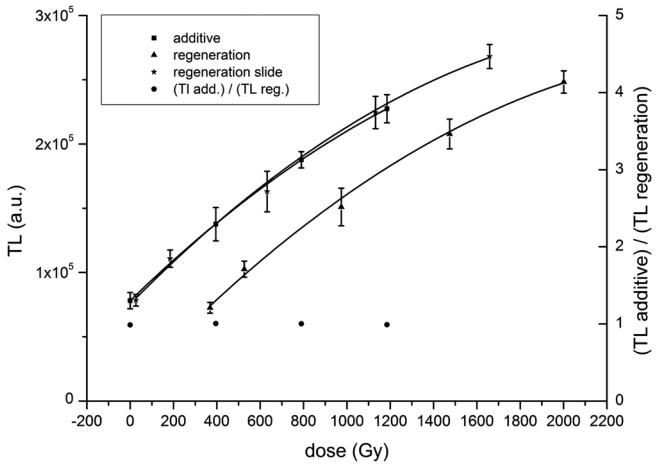

Figure 2 - TL growth curves of sample EVA-LUM-07/29 showing polynomial fits for the additive growth curve (TL add; squares), the regenerated growth curve (TL reg.; triangles) and the shifted regeneration growth curve (TL regeneration slide; stars). The ratio of the two growth curves (TL add. / TL reg.) after shifting is given for the additive doses as grey dots in order to show their similarities in shape ("homothetie" after Mercier (1992).

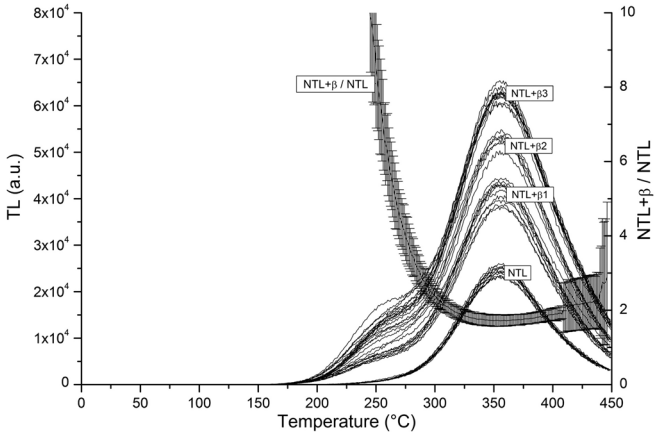

Figure 3 - TL glow curves and heating plateau of sample EVA-LUM-07/32. The natural TL-signals (NTL), the additive TL-signals (NTL+β) and the ratio of NTL+β to NTL over temperature (heating plateau defined as the temperature range of constant ratio) are shown.

Mercier 1991). Between 6 and 12 aliquots were used for each of the 4-5 dose points for each of the two growth curves, where the grains for the regeneration growth curve were heated to 360°C for 90 min in air before irradiation. This procedure is assumed to induce the least sensitivity changes. Carbonates were removed with acetic acid after crushing and/or heating. Thermoluminescence was detected with an 'EMI 9236QA' photomultiplier with detection restricted to the UV-blue wavelength band by Schott BG25 and WG5 filters at a heating rate of 5°C min^{-1} to 450°C on Risø DA-20 or DA-15 systems. Irradiations were performed with external calibrated sources (β with $^{90}Y/^{90}Sr$ at ~0.26 Gy s-1 and a with 241Am at 0.178 μm min^{-1}). The alpha sensitivity (β-value after Bowman & Huntley 1984) was determined by a regeneration approach. The luminescence response of single doses from alpha and beta irradiation to six discs each of 4-11 μm fine grain material (heated prior irradiation in air to 500°C for 30 min) was compared in order to obtain the b-value for each sample. The integration range of all luminescence signals analysed was defined by the range of overlap of the temperature ranges of the heating plateau (fig. 3) with the equivalent dose plateau in order to achieve the most accurate and precise results.

Heated flint sample selection, testing and rejection

A small portion from the outer edge of each heated flint submitted for dating was analysed in order to determine the correct attribution as being heat altered. The physical evidence for the past heating is achieved by analysing the TL response from the natural sample in relation to the TL signal from a portion which has received an additional dose from a calibrated radioactive β-source (natural + dose). The flat ratio (plateau) of the 2 signals over temperature indicates the presence of the prehistoric zeroing of the TL-signal for a given temperature. In cases of the absence of a prehistoric heating or where the heating was less to ~ 400 °C the ratio of the 2 signals is not uniform or might be flat for a short temperature range only. In such cases the lack of a plateau in the range of the peak temperature indicates the insufficiency of the prehistoric heating for TL dating analysis. An additional criterion of prehistoric heating is the presence of a

single peak with a Gaussian like shape (fig. 3), lacking shoulders at either side and the peak occurring in the temperature range between 350 and 380 °C. Only such samples were considered for dating. If the flat ratio extends over the TL peak temperature, a "heating plateau" (after Aitken 1985) is defined and the sample is confirmed to have been sufficiently heated for TL analysis (fig. 3). Such samples were then prepared for full TL analysis (outer 2 mm removed and crushed) and the test was repeated with this extracted material in order to verify that the temperatures achieved in the interior of the sample were sufficient to fully erase the TL-signal and thus full fill a fundamental assumption in TL-dating of heated flint artefacts. Only such samples were subsequently used for dating analysis (tab. 2).

EVA-LUM-No	square	Inv.-No.	x	y	z	layer
05/16	P.4	55	x	x	-8.20	5g
05/17	P.4	56	x	x	-8.20	5g
07/29	N34	430	112.70	33.35	-9.82	6b East
06/29	N35	6	112.76	35.33	-9.69	6b East
05/18	F35	453	105.50	35.50	-10.09	6b East
07/30	H36	33	107.74	36.88	-10.01	6b East
07/31	F35	136	105.50	35.50	-10.09	6b East
07/32	N39	95	112.58	39.41	-10.06	6b East
09/02	N39	57	112.30	39.50	-10.04	6b East
09/03	H 36	31	107.73	36.94	-10.01	6b East
07/33	D29	154	103.00	29.00	-13.65	α-h base
07/34	E30	68	104.00	30.00	-13.65	α-h base
05/19	E30	195	103.00	30.00	-13.65	α-h base
07/35	A28	139	100.00	28.00	-13.65	α-h base

Table 2 - Locations of samples for TL dating (samples lacking precise coordinates were given square coordinates only or just collected).

Dosimetry

The internal dose rates ($\dot{D}_{external}$) were calculated after (Adamiec & Aitken 1998) based on Neutron Activation Analysis results for U, Th and K on 200 mg of sample material less than 160 μm from the extracted cores, which were obtained prior to the chemical treatment.

Dosimetric dating methods are based on the assumption of the stability of the dose rates over the burial time and the homogeneous distribution of radioactive elements in the sample. However, either can be modelled as well (Guibert *et al.* 2009; Tribolo *et al.* 2006). The flint samples from Hummal do not exhibit a large variability of grain sizes on the macroscopic scale and inhomogeneities are therefore unlikely. The stability of the internal dose rates can not be contested over the time range of interest because only those parts were used for analysis which did not show any macroscopical traces of geochemical alterations, like patination.

Most sediments at Hummal consist of fine grained particles and only the archaeological material (lithics and bones), while large clastic input (e.g large pebbles/gravel to cobble) is usually not present. Such sediment layers are not considered as especially "lumpy" and external dosimetry is therefore based on the analysis of the fine parts of the sediments with HpGe-γ-spectrometry (SiO_2 matrix) in the laboratory (tab. 3).

These analyses reveal identical patterns of disequilibria of the ^{238}U decay chain, where concentrations of ^{238}U are always lower than ^{226}Ra, which was found to be the case for all of the sediments at Hummal investigated so far (fig. 4), and which was already detected by Mercier & Valladas (1994) for a sample from a different part of the site as well. The daughter products at the end of the decay chain (e.g. ^{210}Pb) show variable ratios to their mother isotopes. These disequilibria are likely related to the rise and fall of the water table. Fluctuations may be due to natural spring activities or to the lowering of the water table through intensive pumping up of water from the well in the past decades. While HpGe-γ-spectrometry reveals only the present day state, it has to be suspected that disequilibria occurred repeatedly. However, it can not be established how often and when this did happen.

The most plausible interpretation of the occurrence of comparable larger activities measured for some of the ^{238}U daughter products (fig. 4) is uranium leaching (oral communication D. Degering, 2009). Because ^{230}Th is not easily leached, it would represent a good estimate for the dose rate for a recent single leaching of U. Additionally, a recent ^{222}Rn loss could have occurred, as indicated by the lower activity of the daughter product ^{210}Pb. However, ^{226}Ra could have been leached in, and a multiple leaching out of uranium could have occurred, as another scenario amongst others. Modelling the dose-rate for such a scenario would require the knowledge of the age of the sequence and the number of leaching cycles, as well as measurements of all sedimentological units of the stratigraphy in order to place the observed disequilibria in relation to each other. The general assumption of the constancy of dose rates for TL-dating is therefore not valid and age estimates can only be provided for dose rate models based on HpGe-γ-spectrometry. Given this problematic, only borderline model ages can be calculated and they will be restricted to the most likely minimum and maximum age.

layer	^{238}U serie				^{232}Th serie		K
	^{238}U (A/m /Bq/kg)	^{230}Th (A/m /Bq/kg)	^{226}Ra (A/m /Bq/kg)	^{210}Pb (A/m /Bq/kg)	^{228}Ra (A/m /Bq/kg)	^{228}Th (A/m /Bq/kg)	^{40}K (A/m /Bq/kg)
5g	34 ± 3	100 ± 26	78 ± 2	6 ± 3	12 ± 1	12 ± 1	100 ± 3
6b East	29 ± 3	96 ± 21	177 ± 2	131 ± 3	11 ± 1	11 ± 1	124 ± 3
α-h-base	97 ± 4	204 ± 26	324 ± 3	233 ± 5	112 ± 4	115 ± 3	37 ± 2
15b	30 ± 3	81 ± 20	87 ± 2	143 ± 5	7 ± 1	7 ± 1	121 ± 3

Table 3 - Results from HpGe γ-ray spectrometry on dry sediment samples.

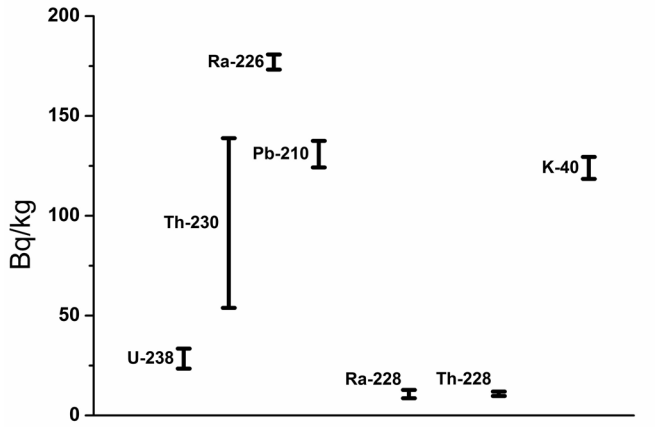

Figure 4 - Results of activity measurements (2s) of the products of the ^{238}U-decay chain with HpGe-g-ray spectrometry (^{234}Th for ^{238}U; ^{214}Pb and ^{214}Bi for ^{226}Ra; ^{230}Th; ^{210}Pb), for ^{40}K and of the ^{232}Th-decay chain (^{212}Pb, ^{212}Bi, ^{208}Tl for ^{228}Th; ^{228}Ra) of the fine grained (<5 cm) component of layer '6b-East'. Note that the sediments from the other layers display a similar general pattern.

layer	min.total γ-dose rate (μGy a^{-1})	max. total γ-dose rate (μGy a^{-1})
5g	482	757
6b East	440	1006
α-h-base	3078	3499
15b	405	832

Table 4 - g-dose-rates (μGy a^{-1}) for dry sediments based on HpGe-γ-ray spectrometry. The minimum γ-dose rate is based on the activity of ^{238}U and the maximum γ-dose-rate on the activity of ^{230}Th. Note that for layer 'α-h-base' only half of the values were used for age calculation because the other 2π relates to the underlying consolidated sediment (table 5). All data is corrected for 10% moisture content of the sediment (15% for 'α-h-base').

A simple scenario would be the single leaching of U, probably related to the recent digging of the well shaft, comparable to a model used by Zander *et al.* (2007). For this scenario the dose-rate would be best represented by ^{238}U as a minimum dose (tab. 4) and calculations based on ^{238}U therefore can be considered as maximum age estimates. The disequilibria between ^{230}Th and ^{226}Ra is often related to recent events (oral communication D. Degering, 2009), and could be linked to the very recent lowering of the water table. ^{230}Th therefore is considered as best representing the maximum dose, thus providing the model for a minimum age estimate (tab. 4). Obviously other and more complex scenarios are possible. However, no data is available to further constrain such models and resulting ages would be within the limits given by the two proposed models. These model ages are based on the values measured for ^{230}Th and ^{238}U, which allow the calculation of total external γ-dose rates, assuming constant dose rates from the U-series.

The assemblage of layer 'α-h-base' was located laying directly on a solid consolidated sediment. Therefore half of the γ-dose-rate derives from this rock material, which was analysed by Neutron Activation Analysis (NAA), presented in table 5. The sum of half the dose rates provided by NAA and HpGe-γ-spectrometry give the γ-dose-rate for the samples from this layer, where minor variations in the basal surface geometry are neglected.

While ^{230}Th is considered as most likely being the best available representative of the past dose-rate, even though providing minimum age estimates only, the results based on ^{234}U have to be considered as absolute minimum rates, and thus maximum possible ages. In laboratory γ-ray spectrometry the dry sediment is analysed. The results therefore have to be corrected for the water (moisture) contained in the sediments. Because of the location in an arid zone, sediment moisture is difficult to be determined in the field. We here assume 10% moisture for the sediments from layers '5g', '6b-East' and '15b', while for layer 'α-h-base' a moisture of 15% is assumed because of the location of the flint samples in the depth of a dolina and lying on a dense and less permeable `rock, which probably acted as a water barrier. An increased water flow in this sediment is evidenced by the presence of SiO_2 deposits on sediment quartz grains and artefacts which require at least episodical water flow for its formation (Shackley 1988). Because the dose rates were not constant and have to be modelled, representativeness of any measurements of the present state is questionable for the past. However, the γ-dose-rate obtained by HpGe-γ-spectrometry for layer '6b-East' (1214 μGy a^{-1}) is comparable to measurements by two *in situ* Al_2O_3:C dosemeters (1197 and 1048 μGy a^{-1}). The small difference can be attributed to differences in moisture content, which would provide a 8 % natural moisture for the averaged dosemeters. This is well comparable with the value of 10% used in age calculation, which was employed in order to compensate for the reduced moisture of the sediments under study here. Uncertainties of a few percent related to the unknown moisture content of the sediments are negligible in the light of the uncertainties related to the spread in ages caused by the modelling of the external γ-dose rate. For the age calculation an uncertainty of 10% was used for the external γ-dose rate. The cosmic dose was estimated by taking into account the geographic position, altitude and thickness of sediments (Prescott & Hutton 1994; Prescott & Stephan 1982), employing a 5% uncertainty (after Barbouti & Rastin 1983).

It is generally assumed that the heating event of lithics from a given archaeological layer was more or less contemporaneous. If this is the case, then the palaeodose-internal dose-rate ratios should fall on a straight line, which is representing the age, whereas the external dose rate is the intercept with the x-axis, because the palaeodose is a function of external and internal dose-rates. Such an approache can sometimes be used to check the external dose rate employed (e.g. Aitken & Valladas 1992).

Optically Stimulated Luminescence Dating of sediment

Layer '15b' is one of several small sand lenses (maximum thickness 15 cm) of aeolian origin, which is embedded in a 10-20 cm package of clay-rich sediments (layer 15). This layer is one of several dark clay layers, which presumably formed in a marshy environment of varying size in depressions of the mound of Hummal. In general, the density of archaeological finds within

the dark clays is very low. The green and black clay deposits are characterised by a high content of organic material and aeolian components (Le Tensorer *et al.* 2007), and therefore the sand lenses in Layer 15 should be well suited for Optically Stimulated Luminescence (OSL) dating.

Method of Optically Stimulated Luminescence Dating

Optically Stimulated Luminescence (OSL) dating is a dosimetric method as well, and the fundamental principles comparable to the ones described above apply. However, the zeroing of the luminescence signal is by light, and therefore the last exposure to light is the event dated. An OSL age therefore can only represent *terminii post quem* or *ante quem* ages for archaeological remains embedded inside, or, as is the case here, below and above the OSL dated layer, for which the timing of its deposition is dated (fig. 5).

OSL measurement parameters and sample preparation

The sample was taken from the sediment profile (square L31, x=110.76, y=31.51, z=-13.03) with a steel tube and the light exposed ends were discarded, but used for HPGe γ-spectrometry. Organic and carbonate materials were removed with H_2O_2 and HCl, respectively, before quartz was separated with heavy liquids. The α-rim was removed by etching in 45% HF, before final sieving (90-160 μm). Feldspar contamination was checked with infrared stimulated luminescence (IRSL) measurements.

The same equipment as for TL was used for measuring the OSL. A single aliquot regeneration (SAR) protocol (Murray & Wintle 2000) was employed to determine the palaeodose. A preheat of 220°C was chosen and the OSL was stimulated for 40 s at 90% power with blue LEDs and the first 0.8 s of the signal was used, while the last 8 s served as a background measurement. The data was analysed with "Analyst 3.24", including the recycling measurement in dose-curve construction, 50 Monte Carlo repeats (Duller 2007), 2% measurement error, while using the previous background (Murray & Wintle 2000). Many data could be only fitted with an exponential+linear function, which was therefore used for all data, because otherwise too few data points would have been available. Failure to regenerate the level of the natural luminescence, as well as recycling ratios deviating by more than 10% from unity; test dose and palaeodose error greater than 15% and 15% max palaeodose error were employed as rejection criteria. A dose recovery test gave 224 ± 4 Gy for 5 natural aliquots which were bleached with blue LEDs for 240 s at 280°C before the dose of 230 Gy was given, thus suggesting that the chosen protocol is capable of determining a given dose very well.

Dosimetry

The problem of disequilibria in the ^{238}U-decay chain was also detected for the sediment from layer '15b (tab. 1) and therefore the discussion above (section 4.5) on the external γ-dose rate applies to OSL samples as well. However, as the quartz grains used for analysis are assumed to be free of any significant radioactive isotopes (following e.g. Henshilwood *et al.* (2002) the external γ-dose rate is of much more importance because no

$$age_{(ka)} = \frac{P_{(Gy)}}{\dot{D}_{(Gy \cdot a^{-1})}} = \frac{P}{\dot{D}_{(external)}} = \frac{P}{\dot{D}_{\beta(U)} + \dot{D}_{\beta(Th)} + \dot{D}_{\beta(K)} + \dot{D}_{\gamma(U)} + \dot{D}_{\gamma(Th)} + \dot{D}_{\gamma(K)} + \dot{D}_{cosmic}}$$

Figure 5 - Age formula for OSL dating, the palaeodose (P) is expressed in Gy, dose rates ($\dot{D}$) in Gy per time unit (usually in a or ka).

stable internal dose-rate is present. Therefore any change on the external γ-dose rate has a large effect on the calculated age. The dose rate for the OSL sample therefore consist of the external β- and γ-radiation, as well as the cosmic dose rate (91 μGy^{-1}), which was calculated as described above. No a-radiation has to be considered because the sample was etched with HF for 45 min.

The sediment lense was thin, and just thick enough to allow the sampling for one OSL sample. The γ-dose rate of 1450 $\mu Gy\ a^{-1}$ measured in the field with a portable NaI-γ-spectrometer (Target NanoSpec) can not be considered as representative, because the sands did not reach much further than the 10 cm sampling depth. Therefore the probe was exposed at 4π (30 cm) depth mainly to the higher radiation from the clayey lacustrine sediments, and not the sands. Therefore the actual γ-dose rate should be between the *in situ* measurement result and the HPGe-γ-ray spectrometry of the sediment which was discarded from either end of the sampling tube. However, given the problem of disequilibria as described above, model ages will be presented based only on HPGe-γ-spectrometry measurements, which were corrected for 10 % moisture. Because the largest HPGe-γ-contribution is from the immediate vicinity of the sample, the laboratory measurement of the sand is assumed to be the best representative data available (tab. 4).

Thermoluminescence (TL) dating results

A total of 60 flints showing signs of having been exposed to fire were tested for the sufficiency of the prehistoric heating with the heating plateau test. We here present the TL dating results on a total of 14 samples which passed this test. Two originate from the Mousterian layer '5g', eight were recovered from the Hummalian layer '6b East', as were four from the Dolina filling (layer 'α-h base').

Table 6 shows the results of the TL measurements as well as Neutron Activation Analysis results. The palaeodoses for the two samples from layer '5g' are in the same order of magnitude, but their internal dose rates are vastly different (tab. 6). A similar picture is observed for the samples from layer '6b East', where two samples (EVA-LUM-07/29 and -09/03) have rather different internal dose rates. For layer 'α-h base' the palaeodoses are not very different, while the internal dose rates exhibit some variation (tab. 6). Samples having been heated at the same time and always located in the same sediment layer are expected to show the same trend of large palaeodoses with high internal dose rates and vice versa. Having been exposed to similar external γ-dose rates, all samples of the same age are expected to cluster along a line (representing the age) for internal dose rate versus palaeodose. Figure 6 shows that for layer '6b East' two samples (EVA-LUM-05/18 and 07/32) have higher and lower internal dose rates, respectively, compared to the majority

	U (ppm)	Th (ppm)	K (%)	γ-dose rate (μGy a^{-1})
consolidated sediment	42.80 ± 1.24	0.60 ± 0.01	0.0755 ± 0. 0037	4883

Table 5 - Results of Neutron Activation Analysis (NAA) of the consolidated sediment on which the artefacts from layer 'a-h-base' were laying and conversion to infinite matrix γ-dose rate (Adamiec & Aitken 1998), of which half the value was used for age calculation.

of samples. It therefore has to be suspected that, at least for sample EVA-LUM-07/32 the heating events, and thus the ages, were not the same, or that the external γ-dose rates were vastly different (fig. 6).

The distribution of internal/palaeodose ratios of the samples from layer 'α-h base' forms two groups (fig. 7), with sample EVA-LUM-07/34 not being consistent with the other samples. Its palaeodose is not compatible with the external γ-dose rates the other samples must have received, because no positive relationship (positive slope) can be established. Therefore it can be suspected that sample EVA-LUM-07/34 is not being associated with the same heating event. However, it can not be ruled out that an inhomogeneous distribution of radioactive elements, which cannot be traced with NAA, is responsible for over or under estimation of the internal dose rates. In contrast, it has to be kept in mind that the external γ-dose rates can be rather different in Palaeolithic sites, because of the heterogeneity of the sediments, and therefore clear relationships between parameters are not necessarily expected.

The dependencies of the calculated ages for either model (tab. 7 and 8) on the external γ-dose rates is large, because the internal dose rates, which can be regarded as having been stable over the entire burial time, range between 5 and 50% of the total dose rate only.

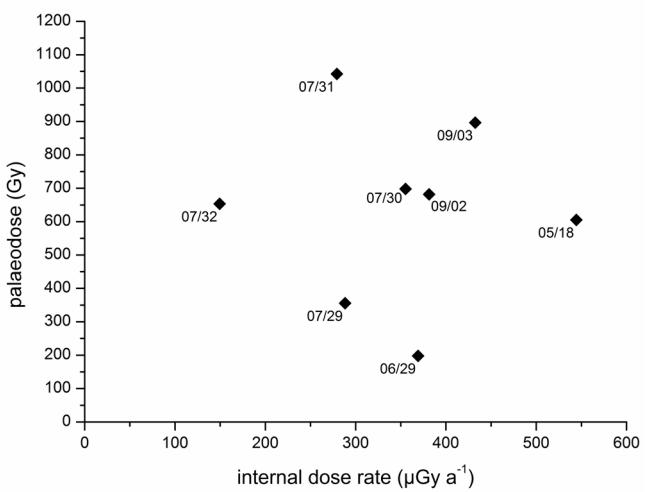

Figure 6 - Internal dose rates versus palaeodoses for samples from layer '6b East'.

The ranges of TL model age estimates for minimum ages (tab. 7) and maximum ages (tab. 8) obtained for the layers of Hummal are very large. While for layer '6b East' the model ages for the individual samples are significantly different (2σ), there are no significant difference for the samples from the other two layers. Therefore modelling has a large effect on the samples from layer '6b East' only.

The age results for layers '6b East' and 'α-h base' pass the Shapiro-Wilk test at p=0.05 (software package Origin 8.1) for both models and therefore are considered to have been drawn each from normal populations. Tests to determine outliers (Dixons test after Rorabacher 1991; Grubb's test; Chauvenet criterion) failed to detect any abnormal results, but all data fails X^2-tests. Therefore we prefer to calculate simple average ages for the samples from one layer, assuming that the heating event was contemporaneous.

EVA-LUM-No	layer	heating plateau (°C)	D_E-plateau (°C)	Palaeodose (Gy)	b-value (Gy μm^2)	U (ppm)	Th (ppm)	K (ppm)	D_{cosmic} (μGy a^{-1})	eff. $D_{internal}$ (μGy a^{-1})
05/16	5g	340-390	330-390	181±6	2.43±0.02	1.28±0.04	0.20±0.01	573±11	120	292±5
05/17	5g	330-410	340-380	132±9	1.82±0.01	2.67±0.05	0.31±0.01	1162±23	120	573±7
07/29	6b East	340-380	350-370	355±19	2.44±0.03	1.10±0.07	0.29±0.03	914±55	147	288±11
06/29	6b East	335-425	340-370	196±6	1.80±0.03	1.67±0.04	0.21±0.01	863±19	147	369±6
05/18	6b East	350-390	340-370	605±33	2.05±0.02	2.71±0.05	0.12±0.01	656±17	147	545±7
07/30	6b East	350-380	340-370	698±26	3.24±0.02	1.40±0.08	0.18±0.02	860±34	147	355±14
07/31	6b East	340-390	350-380	1037±59	2.16±0.01	1.10±0.07	0.29±0.03	869±61	147	279±11
07/32	6b East	340-390	340-365	653±23	1.95±0.02	0.53±0.05	0.21±0.03	602±48	147	149±9
09/02	6b East	340-400	345-375	682±29	2.22±0.02	1.78±0.09	0.22±0.03	598±42	147	381±14
09/03	6b East	340-430	360-400	897±31	2.87±0.03	1.90±0.10	0.22±0.02	699±42	147	433±15
07/33	α-h base	335-425	340-370	694±31	2.53±0.02	2.16±0.05	0.18±0.01	730±15	57	471±8
07/34	α-h base	350-390	340-370	839±46	1.74±0.02	0.67±0.05	0.06±0.01	687±55	57	173±9
05/19	α-h base	330-400	340-370	751±53	1.13±0.01	2.42±0.04	0.27±0.01	755±18	57	467±7
07/35	α-h base	350-380	340-370	543±18	2.32±0.06	0.89±0.06	0.22±0.03	642±51	57	223±10

Table 6 - Results of TL measurements, Neutron Activation Analysis and dosimetry. Uncertainties for $\dot{D}_{g\text{-}ext.eff.}$ is 5%.

EVA-LUM-No	layer	^{230}Th based eff. Dexternal γ (μGy a^{-1})	eff. Dinternal (% total D)	eff. Dexternal γ (% total D)	min. age (ka) based on ^{230}Th
05/16	5g	723	26	64	159±13
05/17	5g	448	41	50	97±7
07/29	6b East	956	21	69	255±22
06/29	6b East	951	25	65	135±11
05/18	6b East	969	33	58	365±29
07/30	6b East	915	25	65	492±40
07/31	6b East	423	33	50	1221±88
07/32	6b East	966	12	77	518±46
09/02	6b East	951	26	64	461±38
09/03	6b East	946	28	62	588±47
07/33	α-h base	3324	12	86	180±18
07/34	α-h base	3359	5	94	234±25
05/19	α-h base	3359	12	87	193±20
07/35	α-h base	3307	6	92	151±15

Table 7 - Minimum age TL dating results for heated flints based on a ^{230}Th derived external γ-dose rate. Uncertainty in age calculation for $\dot{D}_{g\text{-}ext.eff.}$ is 10 % (see text).

EVA-LUM-No	layer	^{234}U based eff. Dexternal γ (μGy a^{-1})	eff. Dinternal (% total D)	eff. Dexternal γ (% total D)	min. age (ka) based on ^{234}U
05/16	5g	723	33	53	206±15
05/17	5g	448	50	39	116±8
07/29	6b East	418	34	49	410±29
06/29	6b East	460	38	47	201±14
05/18	6b East	469	47	40	507±34
07/30	6b East	401	39	44	773±52
07/31	6b East	423	33	50	1221±88
07/32	6b East	423	21	59	916±69
09/02	6b East	416	40	44	715±49
09/03	6b East	414	44	42	901±60
07/33	α-h base	2924	14	85	199±19
07/34	α-h base	2955	5	93	263±13
05/19	α-h base	2955	13	85	216±22
07/35	α-h base	2909	7	91	170±17

Table 8 - Maximum age TL dating results for heated flints based on a ^{234}U derived external γ-dose rate. Uncertainty in age calculation for $\dot{D}_{g\text{-}ext.eff.}$ is 10% (see text).

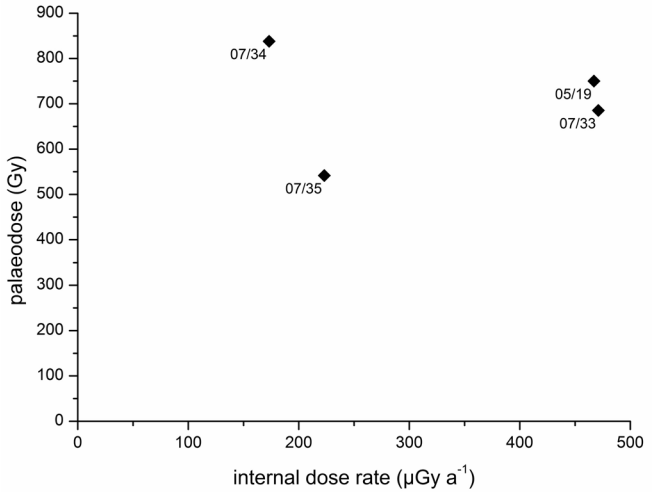

Figure 7 - Internal dose rates versus palaeodoses for samples from layer 'α-h base'.

For layer '5g' only two samples were datable, with rather opposing relationships between dose rates. Results for sample EVA-LUM-05/17 can be considered as more reliable because it is less dependent on the model for the external γ-dose rate. Six flints produced age results for layer '6b East'. The spread in ages is enormous and significant differences are observed between the two models employed. The minimum age model provides a mean age of 445 ± 192 ka (1σ standard deviation), whereas for the maximum age it is 706 ± 324 ka for all samples. The two samples (EVA-LUM-05/18 and -07/32) which were suspected of not belonging to the same population actually provide ages rather close to this mean and therefore the argument is not supported by the apparent ages. The mean results on the four heated flints from layer 'α-h base' provide 190 ± 35 ka as minimum context age estimate, and 210 ± 40 ka (1σ standard deviation) for maximum age. Here again the calculated age for the suspected sample (EVA-LUM-07/34) is relatively close to the mean, suggesting that it belongs to the majority of sampled artefacts, despite having apparently experienced a different dosimetry.

Optically Stimulated Luminescence (OSL) Dating results

A total of 48 aliquots were measured for sample EVA-LUM-08/16, of which 12 were rejected according to the criteria stated above. The data does not show any distinct pattern, but a rather wide dose distribution (fig. 8), which is difficult to interpret for aeolian sediments, which should be represented by a rather defined distribution. The resulting palaeodose based on the weighted mean of 228 Gy is not distinctively different from the radial plot result where 69% of the data are encompassed within 2σ, giving 246 Gy. Subsequently, the weighted mean palaeodose of 228 ± 36 Gy was used for the age calculation of sample EVA-LUM-08/16.

Based on the dosimetry discussion above, a maximum age of the deposition of the sand lens '15b' can be calculated by employing a γ-dose rate derived from the HpGe γ-spectrometry measurement of ^{238}U (tab. 3) and by assuming this value to represent an average minimum dose the sample has received. Vice versa a minimum age can be calculated based on ^{238}Th and the resulting ages for sample EVA-LUM-08/16 are 203 ± 36 ka and 111 ± 27 ka, respectively.

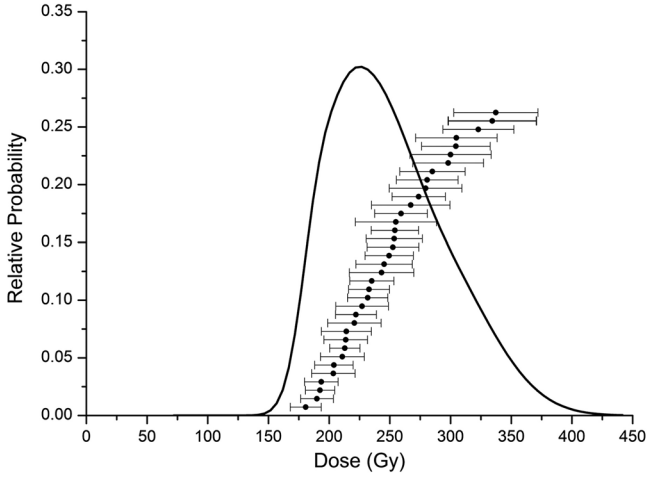

Figure 8 - Probability distribution of equivalent doses (DE) obtained for sample EVA-LUM-08/16.

Discussion of TL ages

The two models for the external γ-dose rate do not produce significantly different results for the samples from layer '5g'. However, the ages of the two samples are significantly different, which might indicate that two occupations were sampled, which are significantly different in time. Sample EVA-LUM-05/17 is less dependent on the γ-dose rate and therefore appears to be more reliable. Furthermore, with an age of approximately 100 ka it is in accordance with age estimates for similar Mousterian assemblages. However, given the large spread in TL ages of heated flint (see discussion above and e.g. Richter *et al.* 2010) such a single age estimate can not be taken as a good estimate for the age of an entire assemblage and is rather providing a general idea on the age of the layer only.

Significantly different results are obtained for the two external γ-dose rate models for the samples from layer '6b East'. While the maximum age model can be clearly rejected as being too old on archaeological arguments, the minimum age model does not fit the chronostratigraphical models (Bar-Yosef & Meignen 2001; Porat *et al.* 2002) of the Levant either. The data appears to represent different heating events or vastly different dose rates because of the enormous spread in TL-ages, which is not reflected in the proportional relationship of palaeodoses to internal dose rates. Considering that the assemblage shows clear signs of diagenetic modifications (surface exposure and trampling), but is a rather uniform assemblage in technological and typological terms (Le Tensorer *et al.* 2003), it is more likely that different dose rates are the responsible agents. In fact, the artefact assemblage is very similar to the assemblage from layer 'α-h base'. However, because none of the samples dated is typo-technological significant, it can not be ruled out that some samples originate from different assemblages. This TL data suggests that either different assemblages are mixed, or the assemblage has experienced a different dosimetric history than the one assumed. The latter would be the most parsimonious explanation because of the evidence of surface exposure in the form of patiniation and the apparent homogeneity of the assemblage. However, this can neither be quantified nor qualified.

All but one of the samples from layer '6b East' have internal dose rates and palaeodoses rather similar to the samples from layer 'α-h base' (tab. 6). Assuming an external γ-dose rate based on the measurement of solely the sediment from layer 'α-h base', the minimum age model would provide a mean of about 190 ka and the maximum age would be approximately 250 ka. These ages are very similar to the ones obtained for layer 'α-h base' and provide further evidence, that the external γ-dose rate models are likely not appropriate for the samples from layer '6b East'. A significant difference in ages is observed to the previous TL study whatever scenario is applied to the data presented here, despite the correlation of the location of layer VIb to the present day stratigraphy with layer '6b-East'. However, as outlined above, these previous age estimates (Ancient TL date list 1988) are considered as underestimations.

The models for the external γ-dose rate do not produce significantly different results for the samples from layer 'α-h base' and the spread in ages is comparable to TL-dating of other middle Palaeolithic sites. Because of the lack of age differences for the two models and under the assumption that the artefacts were re-deposited into the dolina quickly after their original deposition, it can be concluded that the age of this assemblage is ca. 200 ka (minimum model 190 ± 35 ka and maximum model 210 ± 40 ka), which fits very well the chronostratigraphical interpretation of the Levant (Mercier & Valladas 2003; Mercier *et al.* 1995b, 2000, 2007; Rink *et al.* 2003).

Discussion of the OSL age

The large influence of the γ-dose rate in OSL dating is evidenced by the two model ages for sample EVA-LUM-08/16 of 203 ± 36 ka and 111 ± 27 ka. However, these results are statistically identical at 98% probability (2σ). Furthermore, the stratigraphic location of the layer with respect to the TL dating results of selected archaeological layers above, as well as the overall chronostratigraphic interpretation of the site (layer 15 being older than ~ 350 ka, Le Tensorer *et al.* 2011), indicates a potential underestimation of the age by the presented OSL data. Despite its large palaeodose, the luminescence signal was well below saturation for the accepted aliquots. It is known that OSL ages on quartz might underestimate the age in comparison to e.g. IRSL dating (e.g. Steffen *et al.* 2009). A different explanation might be provided by the detection of authigenic quartz, which formed in a similar environment in the site of Nadaouiyeh Aïn Askar (Pümpin 2003), and which was observed in some limited analysis at Hummal as well. The *in situ* formation of authigenic quartz in deposited sediments requires time (Pümpin 2003), especially as crystals up to 1 mm in size were found. It can occur repeatedly and it is not possible to determine a time frame of formation. The, more or less, continuous palaeodose distribution of the sediment from Hummal could be explained by an intermittent but frequent formation of authigenic quartz for some time after deposition of the sediment. This process could have started rather soon after deposition or occurred later, or even repeatedly. It is not possible to distinguish the palaeodose data from quartz which was bleached and quartz which was formed after deposition. Multigrain aliquots could contain grains from different populations and therefore a continuous palaeodose distribution could be generated as a result

of this mixing, which can not be distinguished from continuous formation over a certain period. Single grain luminescence analysis is required to investigate this hypothesis, by measuring palaeodoses from isolated single authigenic quartz and aeolian grains. If formation happened at different times or significantly after deposition, it might be possible to distinguish different palaeodose populations. However, it would be difficult to separate aeolian grains with attached (or coated) secondary quartz formation from single isolated authigenic quartz for grain numbers required for single grain OSL dating. Attempts to investigate differences in dissolution rates of aeolian versus authigenic quartz are under way, which might allow the separation of these quartz populations.

Based on this hypothesis, it might be assumed that the largest palaeodoses of around 330 Gy reflect the depositional age better, because the aeolian grains should have received the largest doses. However, this would be a minimum estimate again because multiple grain aliquots were measured. Hypothetical calculations for the two γ-dose rate models give ages of 160 ± 35 ka and 294 ± 39 ka for sample EVA-LUM-08/16, which are not significantly older than the ages based on weighted average palaeodoses.

Conclusions

The occurrence of disequilibria in the U-decay chain enforces the modelling of the external γ-dose-rates for dosimetric dating of the site of Hummal. The resulting TL-ages are significantly different for layers '5g' and '6b East', but not for layer 'α-h base'. Layer 'α-h base' is archaeologically not *in situ* and though layer '5g' and '6b' are documented within the stratigraphical sequence, both were exposed on the surface over certain time. Therefore the association of all samples to single archaeological events can be questioned. However, this appears to be less of a problem for the catastrophic displacement of the artefacts into layer 'α-h base', because consistent age results were obtained. This is in contrast to the two other layers, where for layer '5g' an age of approximately 100 ka is concluded from one result only, because of its increased reliability based on a larger internal dose-rate (considered as stable over burial time) in contrast to the other result. Furthermore, this age is also more in accordance with age estimates obtained for similar Tabun C type assemblages like Tabun unit I (Grün & Stringer 2000; Mercier & Valladas 2003), Skhul B (Mercier *et al.* 1993) and the Qafzeh material (Schwarcz *et al.* 1988; Valladas *et al.* 1988). The large discrepancies in model ages obtained for the two artefacts from layer '5g' indicate that the dose rate models are not appropriate for all samples from this layer, or that different events were dated.

These problems are becoming even more evident for the TL-age results for layer '6b East' which are too inconsistent to be associated with heating events close in time. While the archaeology is not consistent with an accumulation over an extended period of time, it has to be suspected that external dose rates apply, which are different to the one assumed here for establishing ages. Changes in the sediment surrounding the samples, in addition to the surface exposure, can be suspected as the cause. The resulting ages are likely overestimated, especially in the light of the dating results obtained for the other Hummalian assemblage and similar industries (see below). However, comparable results would be obtained if the external γ-dose-rate model from the sediment of layer 'α-h base' would be employed, which is also attributed to the Hummalian. It can be suspected that the changes in sediments and a potential small scale re-depositioning of the artefacts from layer '6b East' took place much later compared to 'α-h base'. However, the TL-dating results for layer '6b East' are considered as unreliable and therefore rejected.

The context age estimate of approximately 200 ka (minimum model 190 ± 35 ka and maximum model 210 ± 40 ka), as an average estimate for the heated flints from layer 'α-h base' compares well with age estimates for similar blade-rich Middle Palaeolithic industries, like Hayonim layer 'F top' and 'F base' with mean TL-dates on heated flint of 210 ± 28 ka and 221 ± 21 ka, respectively (Mercier *et al.* 2007), or at Tabun for unit IX (Tabun D-type) of 256 ± 26 ka with the same method (Mercier & Valladas 2003) with compatible Early Uptake ESR-dates on animal teeth (Grün & Stringer 2000). The agreement of the TL-ages for 'α-h base' at Hummal with these age estimates can be taken as indirect evidence that the model of a short time interval between original and re-deposition of the artefacts from 'α-h base' appears to be correct. However, the results for layer '6b East' do not agree with the previous attempts to date artefacts from this layer (see above). The results presented here appear to confirm the criticism raised above and by Mercier and Valladas (1994), stating that these previous age estimates are likely age underestimations.

The apparent age underestimation by OSL is likely caused by the post-depositional *in situ* formation of authigenic quartz. To our knowledge the formation of authigenic quartz in deposits has so far not been suggested as an explanation for age underestimation and observed palaeodose distribution in quartz OSL dating. The young OSL age, independent of the dose rate model, is neither compatible with the chronostratigraphy nor with the TL ages. This leads to the rejection of this OSL age because of suspicion that the underestimation is caused by the inclusion of authigenic quartz in the multi grain analysis.

Despite the problems in establishing the appropriate dose-rates for dosimetric dating at the site of Hummal, the modelled results for layer 'α-h base' indicate, that these problems can have little influence on the results, because the differences for the two models are not significant. This is promising in the light of the ongoing dating attempts for the Mousterian layers, which are mostly *in situ*. The interpretation of the sedimentological sequence and the state of the archaeological content of layer 'α-h base' appear to be correct, as shown by its TL age of approximately 200 ka which is in accordance with chronometric dating results on similar assemblages from the Near East.

Acknowledgements

S. Albert (MPI-EVA) is thanked for preparing and TL measuring the flint samples, D. Degering (VKTA) for γ-ray spectrometry and T.Schiffer (CEZ) for Neutron Activation Analysis. This research was made possible with the financial aid of: the Swiss

National Foundation, the Freiwillige Akademische Gesellschaft Basel and the Tell Arida Foundation, as well as a travel grant by the Leakey Foundation to Daniel Richter. We are grateful to the General Directorate of Antiquities and Museums of Syria for permission and assistance in carrying out our work, this gratitude is also extended to the Palmyra Museum for its help in our research. We also thank all members of the excavation team in Hummal, and the local community for their support.

References

(1988) - Ancient TL date list 2. *Ancient TL* Supplement, 26.

Adamiec G. & Aitken M.J. (1998) - Dose-rate conversion factors: update. *Ancient TL* 16: 37-50.

Aitken M.J. (1985) - *Thermoluminescence Dating*. London, Academic Press.

Aitken M.J. & Valladas H. (1992) - Luminescence dating relevant to human origins. *Philosophical Transactions of the Royal Society of London Series B: Biological Sciences* 337:139-144.

Aitken M.J. (1998) - *An Introduction to Optical Dating. The Dating of Quaternary Sediments by the Use of Photon-stimulated Luminescence*. Oxford, Oxford University Press.

Alperson-Afil N., Richter D., Goren-Inbar N. (2007) - Phantom hearths and the use of fire at Gesher Benot Ya'aqov, Israel. *PaleoAnthropology* 2007:1-15.

Bar-Yosef O. (1998) - The Chronology of the Middle Paleolithic of the Levant. In: T. Akazawa, K. Aoki, O. Bar-Yosef (eds.), *Neandertals and Modern Humans in Western Asia. New York*, Plenum Press, p. 39-56.

Bar-Yosef O. & Meignen L. (2001) - The Chronology of the Levantine Middle Palaeolithic Period in Retrospect. *Bulletins et mémoires de la Société d'Anthropologie de Paris 13*:269-289.

Barbouti A.I. & Rastin B.C. (1983) - A study of the absolute intensity of muons at sea level and under various thickness absorber. *Journal of Physics G: Nuclear Physics* 9:1577-1595.

Barkai R., Gopher A., Lauritzen S.E., Frumkin A. (2003) - Uranium series dates from Qesem Cave, Israel, and the end of the Lower Palaeolithic. *Nature* 423:977-979.

Bellomo R.V. (1993) - A methodological approach for identifying archaeological evidence of fire resulting from human activities. *Journal of Archaeological Science* 20:525-553.

Bøtter-Jensen L., Mckeever S.W.S., Wintle A.G. (2003) - *Optically Stimulated Luminescence Dosimetry*. Amsterdam, Elsevier.

Bowman S.G.E. & Huntley D.J. (1984) - A new proposal for the expression of alpha efficiency in TL dating. *Ancient TL* 2:6-8.

Duller G.A.T. (2007) - Assessing the error on equivalent dose estimates derived from single aliquot regenerative dose measurements. *Ancient TL* 25:15-24.

Gopher A., Ayalon A., Bar-Matthews M., Barkai R., Frumkin A., Karkanas P., Shahack-Gross R. (2010) - The chronology of the late Lower Paleolithic in the Levant based on U-Th ages of speleothems from Qesem Cave, Israel. *Quaternary Geochronology* 5:644-656.

Grün R. & Stringer C.B. (2000) - Tabun revisited: revised ESR chronology and new ESR and U-series analyses of dental material from Tabun C1. *Journal of Human Evolution* 39:601-612.

Guibert P., Lahaye C., Bechtel F. (2009) - The importance of U-series disequilibrium of sediments in luminescence dating: A case study at the Roc de Marsal Cave (Dordogne, France). *Radiation Measurements* 44:223-231.

Hauck T. (2010) - *The Mousterian sequence of Hummal (Syria)*. PhD-Dissertation, Basel, Universität Basel.

Hauck Th. (2011) - The Mousterian sequence of Hummal and its tentative placement in the Levantine Middle Paleolithic. In: J.-M. Le Tensorer, R. Jagher, M. Otte (eds.), *The Lower and Middle Palaeolithic in the Middle East and Neighbouring Regions*. Liège, ERAUL 126:309-323.

Hauck T., Wojtczak D., Wegmüller F., Le Tensorer J.-M. (2010) - Variation in Lower and Middle Palaeolithic land use strategies in the Syrian Desert steppe: The example of Hummal (El Kowm area). In: N.J. Conard & A. Delagne (eds.), *Settlement Dynamics of the Middle Paleolithic and Middle Stone Age - Volume III*. Tübingen, Kerns Verlag, p. 145-162.

Hennig G.J. & Hours F. (1982) - Dates pour le passages entre l'Acheuléen et le Paléolithique moyen à El Kowm (Syrie). *Paléorient* 8:81-83.

Henshilwood C.S., D'Errico F., Yates R., Jacobs Z., Tribolo C., Duller G.A.T., Mercier N., Sealy J.C., Valladas H., Watts I., Wintle A.G. (2002) - Emergence of modern human behaviour: Middle Stone Age engravings from South Africa. *Science* 295:1278-1280.

Herz N. & Garrison E.G. (1998) - *Geological Methods for Archaeology*. Oxford, Oxford University Press.

Hours F. (1982) - Une nouvelle industrie en Syrie entre l'Acheuléen et le Levalloiso-Moustérien. *Archéologie au Levant, Recueil à la mémoire de Roger Saidah*. Lyon, Maison de l'Orient, p. 33-46.

Le Tensorer J.-M., Hauck T., Wojtczak D. (2003) - Le Paléolithique ancien et moyen d'Hummal (El Kowm, Syrie centrale). *Swiatowit* V(B):45-52.

Le Tensorer J.-M. (2004) - Nouvelles fouilles à Hummal (El Kowm, Syrie centrale) premiers résultats (1997-2001). In: O. Aurenche, M.L. Mière, P. Sanlaville (eds.), *From the River to the Sea - The Palaeolithic and the Neolithic on the Euphrates and in the Northern Levant*. BAR International Series 1263:223-240.

Le Tensorer J.-M., Jagher R., Rentzel P., Hauck T., Ismail-Meyer K., Pümpin C., Wojtczak D. (2007) - Long-term site formation processes at the natural springs Nadaouiyeh and Hummal in the El Kowm Oasis, Central Syria. *Geoarchaeology* 22:621-640.

Le Tensorer J.-M., von Falkenstein V., Le Tensorer H., Muhesen S. (2011) - Hummal: a very long Paleolithic sequence in the steppe of central Syria – considerations on Lower Paleolithic and the beginning of Middle Paleolithic. In: J.-M. Le Tensorer, R. Jagher, M. Otte (eds.), *The Lower and Middle Palaeolithic in the Middle East and Neighbouring Regions*. Liège, ERAUL 126:235-248.

Masson A. (1982) - Les pièces lustrées des sources d'El Kowm (Syrie). *Cahiers de l'Euphrate* 3:141-147.

Meignen L. (2007) - Le phénomène laminaire au Proche-Orient, du Paléolithique inférieur aux débuts du Paléolithique supérieur. In: J. Evin (ed.), *Un siècle de construction du discours scientifique en Préhistoire, 3, Aux conceptions d'aujourd'hui*. Actes du Congrès Préhistorique de France, XXVIe session, Congrès du Centenaire, 21-25 septembre 2004, Avignon, p. 79-94.

Mercier N. (1991) - Flint palaeodose determination at the onset of saturation. *Nuclear Tracks and Radiation Measurements* 18:77-79.

Mercier N. (1992) - *Apport des méthodes radionucleaires de datation a l'étude du peuplement de l'Europe et du Proche-Orient au cours du Pleistocène moyen et supérieur*. Thèse, Bordeaux, Université de Bordeaux I.

Mercier N., Valladas H., Bar-Yosef O., Vandermeersch B., Stringer C.B., Joron J.L. (1993) - Thermoluminescence date for the mousterian burial site of Es-Skhul, Mt. Carmel. *Journal of Archaeological Science* 20:169-174.

Mercier N. & Valladas H. (1994) - Thermoluminescence dates for the palaeolithic Levant. In: O. Bar-Yosef & R.S. Kra (eds.), *Late Quaternary Chronology and Paleoclimates of the Eastern Mediterranean*, p. 13-20.

Mercier N., Valladas H., Valladas G. (1995a) - Flint thermoluminescence dates from the CFR laboratory at Gif: Contributions to the study of the chronology of the middle palaeolithic. *Quaternary Science Reviews* 14:351-364.

Mercier N., Valladas H., Valladas G., Jelinek A.J., Meignen L., Reyss J.L., Joron J.L. (1995b) - TL dates of burnt flints from Jelinek's excavations at Tabun and their implications. *Journal of Archaeological Science* 22:495-509.

Mercier N., Valladas H., Froget L., Joron J.L., Ronen A. (2000) - Datation par thermoluminescence de la base du gisement paléolithique de Tabun (Mont Carmel, Israël). *Comptes Rendus de l'Academie des Sciences Paris; Sciences de la Terre et des Planètes* II:731-738.

Mercier N. & Valladas H. (2003) - Reassessment of TL age estimates of burnt flints from the Paleolithic site of Tabun Cave, Israel. *Journal of Human Evolution* 45: 401-409.

Mercier N., Valladas H., Froget L., Joron J.L., Reyss J.L., Weiner S., Goldberg P., Meignen L., Bar-Yosef O., Belfer-Cohen A., Chech M., Kuhn S.L., Stiner M.C., Tillier A.M., Arensburg B., Vandermeersch B. (2007) - Hayonim Cave: TL-based chronology for this Levantine Mousterian sequence. *Journal of Archaeological Science* 34: 1064-1077.

Meyer K. (2001) - *Mikromorphologische Untersuchungen an Ablagerungen der artesischen Quelle Hummal, Syrien*. Unpublished Diploma Thesis, Basel, Universität Basel.

Murray A.S. & Wintle A.G. (2000) - Luminescence dating of quartz using an improved single-aliquot regenerative-dose protocol. *Radiation Measurements* 32:57-73.

Neuville R. (1951) - *Le Paléolithique et le Mésolithique du désert de Judée*. Paris, Masson et Cie.

Porat N., Chazan M., Schwarcz H.P., Kolska Horwitz L. (2002) - Timing of the Lower to Middle Paleolithic boundary: new dates from the Levant. *Journal of Human Evolution* 43:107-122.

Prescott J.R. & Stephan L.G. (1982) - The contribution of cosmic radiation to the environmental dose for TL dating. Latitude, altitude and depth dependances. PACT, *Revue du groupe européen d'études pour les techniques physiques, chimiques et mathématiques appliquées à l'archéologie* 6:17-25.

Prescott J.R., Huntley D.J., Hutton J.T. (1993) - Estimation of equivalent dose in thermoluminescence dating - the 'Australian slide method'. *Ancient TL* 11:1-5.

Prescott J.R. & Hutton J.T. (1994) - Cosmic ray contributions to dose rates for luminescence and ESR dating: large depths and long-term variations. *Radiation Measurements* 23:497-500.

Pümpin C. (2003) - *Geoarchäologische Untersuchungen an der pleistozänen Fundstelle von Nadaouiyeh Aïn Askar (Syrien)*. Unpublished Diploma Thesis, Basel, Universität Basel.

Richter D. (2007) - Advantages and limitations of thermoluminescence dating of heated flint from Paleolithic sites. *Geoarchaeology* 22:671-683.

Richter D., Moser J., Nami M., Eiwanger J., Mikdad A. (2010) - New chronometric data from Ifri n'Ammar (Morocco) and the chronostratigraphy of the Middle Palaeolithic in the Western Maghreb. *Journal of Human Evolution* 59:672-679.

Rink W.J., Richter D., Schwarcz H.P., Marks A.E., Monigal K., Kaufman D. (2003) - Age of the Middle Palaeolithic Site of Rosh Ein Mor, Central Negev, Israel: Implications for the Age Range of the Early Levantine Mousterian of the Levantine Corridor. *Journal of Archaeological Science* 30:195-204.

Rorabacher D.B. (1991) - Statistical treatment for rejection of deviant values: critical values of Dixon's "Q" parameter and related subrange ratios at the 95% confidence level. *Analytical Chemistry* 63:139-146.

Sanzelle S., Miallier D., Pilleyre T., Faïn J., Montret M. (1996) - A new slide technique for regressing TL/ESR dose response curves - Intercomparison with other techniques. *Radiation Measurements* 26:631-638.

Schwarcz H.P., Gruen R., Vandermeersch B., Bar-Yosef O., Valladas H., Tchernov E. (1988) - ESR dates for the hominid burial site of Qafzeh in Israel. *Journal of Human Evolution* 17:733-737.

Schwarcz H.P. (1994) - Current challenges to ESR dating. *Quaternary Science Reviews* 13:601-605.

Shackley M.L. (1988) - Hot Springs and Glazed Flints: a Controversial Phenomenon Observed on Spring-Mound Artefacts in the Near East. *Levant* 20:119-126.

Steffen D., Preusser F., Schlunegger F. (2009) - OSL quartz age underestimation due to unstable signal components. *Quaternary Geochronology* 4:353-362.

Tribolo C., Mercier N., Selo M., Valladas H., Joron J.L., Reyss J.L., Henshilwood C., Sealy J., Yates R. (2006) - TL dating of burnt lithics from Blombos Cave (South Africa): Further evidence fro the antiquity of modern human behaviour. *Archaeometry* 48:341-357.

Valladas G. & Gillot P.Y. (1978) - Dating of the Olby lava flow using heated quartz pebbles: some problems. PACT, *Revue du groupe européen d'études pour les techniques physiques, chimiques et mathématiques appliquées à l'archéologie* 2:141-150.

Valladas H., Reyss J.L., Joron J.L., Valladas G., Bar-Yosef O., Vandermeersch B. (1988) - Thermoluminescence dating of mousterian 'Proto-Cro-Magnon' remains from Israel and the origin of modern man. *Nature* 331:614-616.

Wagner G.A. (1998) - *Age Determination of Young Rocks and Artifacts*. Berlin, Springer.

Wegmüller F. (2011) - The Lower Palaeolithic assemblage of Hummal. In: J.-M. Le Tensorer, R. Jagher, M. Otte (eds.), *The Lower and Middle Palaeolithic in the Middle East and Neighbouring Regions*. Liège, ERAUL 126:271-278.

Wintle A.G., & Aitken M.J. (1977) - Thermoluminescence dating of burnt flint: application to a Lower Palaeolithic site, Terra Amata. *Archaeometry* 19:111-130.

Wojtczak D. (2011) - Humma (Central Syria) and its Eponymous Industry. In: J.-M. Le Tensorer, R. Jagher, M. Otte (eds.), *The Lower and Middle Palaeolithic in the Middle East and Neighbouring Regions*. Liège, ERAUL 126:289-307.

Zander A., Degering D., Preusser F., Kasper H.U., Bruckner H. (2007) - Optically stimulated luminescence dating of sublittoral and intertidal sediments from Dubai, UAE: Radioactive disequilibria in the uranium decay series. *Quaternary Geochronology* 2:123-128.